JOURNAL OF APPLIED ELECTROCHEMISTRY 23 (1993) 1175–1180

# Electrodissolution of aluminium thin film microband electrodes

E. J. LEE, S.-I. PYUN

*Department of Materials Science and Engineering, Korea Advanced Institute of Science and Technology, Yusong-Gu, Daejon 305-701 Korea*

Received 19 November 1992; revised 9 February 1993

This paper discusses the electrodissolution of aluminium thin films as microband electrodes (length = $5 \times 10^{-3}$ m) in terms of mass transfer determined by voltammetry and a.c.-impedance techniques as a function of bandwidth (20 to 2000 nm) in 0.1 M NaOH solution. The anodic polarization curves of the aluminium microband electrodes show that current density is enhanced with decreasing bandwidth. The ac impedance response suggests that a steady-state diffusion layer appears the more markedly, the smaller the bandwidth. The anodic polarization curves are analysed on the basis of the combined Butler–Volmer high field approximation and the semi-cylindrical diffusion field approximation. As a result of the analysis, the electrodissolution proceeds by a mixed kinetic-mass transfer controlled reaction. The analysis also makes it possible to distinguish the semi-cylindrical diffusive mass transfer contribution to the electrodissolution from the kinetic contribution, i.e., mass transfer index linearly diminishes with decreasing bandwidth. The increased current density is attributable to the decreased mass transfer contribution, i.e., the more predominant semi-cylindrical diffusive mass transfer as compared to laminar diffusive mass transfer.

**Nomenclature**

$k_a$ anodic kinetic constant
$k_c$ cathodic kinetic constant
$F$ Faraday constant
$\alpha_a$ kinetic transfer coefficient for anodic reaction
$\alpha_c$ kinetic transfer coefficient for cathodic reaction
$c^S$ surface concentration
$V$ anodic polarization
$D$ diffusion coefficient
$d$ diffusion layer thickness
$z$ number of electrons transferred
$l$ length of microband electrode
$w$ bandwidth of microband electrode
$r$ radius of cylinder

## 1. Introduction

Aluminium based thin films are commonly used as electronic conductors on silicon integrated circuits (IC) in microelectronic structures. The susceptibility to corrosion in aggressive environments determines the life time of the IC system. The electrodissolution of aluminium based alloys has been extensively studied in various aqueous electrolytes for life time prediction in practical systems using a macroelectrode. In general, dissolution rate on aluminium alloy macroelectrodes is largely controlled by the rate at which dissolved ions are removed from the electrode surface by convection and diffusion [1–4]. A question arises as to how the electrodissolution of aluminium alloys proceeds from the electrode surface on a microscopic scale. The diffusional flux to the microelectrode for a cathodic process is greatly enhanced as compared to the macroelectrode, since the contribution of two- or three-dimensional diffusion, rather than linear diffusion, is considerably enhanced with decreasing dimension of the microelectrode [5–8].

Therefore it is expected that results for macroelectrodes do not give information about dissolution rate or corrosion rate of the aluminium thin film on a microscopic scale. Considering that electrode kinetics are independent of specimen dimension, it is possible to distinguish the mass transfer from the kinetic contribution to the anodic dissolution current of aluminium thin films by using microelectrodes.

The present paper is aimed at examining how diffusional mass transfer from a microband aluminium electrode, as a function of bandwidth, affects the anodic dissolution of aluminium thin films in alkaline aqueous solution. For this purpose, potentiodynamic polarization and ac-impedance measurements were performed on aluminium microband electrodes. The experimental results obtained were analyzed on the basis of the combined Butler–Volmer high field approximation and semi-cylindrical diffusion field approximation.

## 2. Experimental details

Aluminium thin films were coated onto an insulating silicon oxide to thicknesses ranging from 20 to 2000 nm by a conventional sputtering technique. The Al/silicon oxide was then sealed in polyethylene resin. The assembly was polished to expose the cross

0021-891X © 1993 Chapman & Hall

section of the aluminium films. The specimen was ground with successively finer silicon carbide paper, ending with 1200 grit and was finally polished with 0.05 $\mu$m $Al_2O_3$ powder on wet cloth. The edge of this assembly was employed as an aluminium microband electrode, which was characterized by a submicroscopic bandwidth (20–2000 nm) and a macroscopic length of 0.5 cm (Fig. 1).

Electrochemical experiments were conducted in a EG&G Model KO 235 flat cell. The working electrode was the aluminium microband electrode, and a platinum mesh and a saturated calomel electrode (SCE) were used as the counter electrode and reference electrode, respectively. The electrolyte was 0.1 M NaOH solution, previously deaerated for 24 h and agitated by bubbling with purified nitrogen throughout the experiments.

Potentiodynamic polarization experiments were conducted on aluminium microband electrode at a scan rate of 0.2 mV $s^{-1}$ in the potential range −1400 to −900 mV vs SCE after a 2 h exposure at open circuit in order to activate the specimen surface, using a EG&G Model 273 potentiostat. The open circuit potential was found to be about −1040 mV vs SCE.

Electrochemical impedance spectroscopy (EIS) was performed on the aluminium microband electrode with a Solartron model 1255 frequency response analyser in conjunction with a Solartron model 1286 potentiostat by superimposing an a.c. voltage of 5 mV amplitude on a dc potential over the frequency range $10^{-2}$ to $10^4$ Hz. The dc potentials applied to the specimen were an anodic potential of −900 mV vs SCE and a cathodic potential of −1350 mV vs SCE.

## 3. Theoretical background

When aluminium is exposed to an aqueous electrolyte, the hydrated aluminium ion, $Al(H_2O)_6^{3+}$, is rapidly formed, equilibrium being achieved in about 1 $\mu$s [9].

$$Al + 6H_2O = Al(H_2O)_6^{3+} + 3e^- \quad (1)$$

The current density for aluminium dissolution, $i$, is described by the Butler–Volmer relationship [10]

$$i = k_a F \exp(\alpha_a FV/RT) - k_c c^s \exp(-\alpha_c FV/RT) \quad (2)$$

The steady state flux of $Al(H_2O)_6^{3+}$, $n$, through a diffusion layer from the electrode may be expressed as

$$n = Dc^s/d \quad (3)$$

From Equations 2 and 3, and using

$$n = i/F \quad (4)$$

$$i = \frac{k_a F \exp(\alpha_a FV/RT)}{1 + \frac{K_c d}{D} \exp(-\alpha_c FV/RT)} \quad (5)$$

Equation 5 describes the current–potential behaviour for electrodissolution of aluminium and provides two limiting cases concerning the kinetic and mass transfer effects. First, when the second term in the denominator of Equation 5 is much smaller than the first, $i$ is given by

$$i = k_a F \exp(\alpha_a FV/RT) \quad (6)$$

This represents the kinetic contribution to the current density in the absence of mass transfer effects. Secondly, in the case where the second term is much larger than the first, $i$ is given by

$$i = \frac{k_a FD}{k_c d} \exp\left[\frac{(\alpha_a + \alpha_c)FV}{RT}\right] \quad (7)$$

Equation 7 describes the limiting behaviour when the dissolution is mass transfer controlled. It can be therefore said that the second term in the denominator of Equation 5 gives an indication of the extent of the mass transfer effect for a mixed kinetic-mass transfer controlled reaction and furthermore permits separation between kinetic and mass transfer effects. An increase in the mass transfer effect reduces the current density.

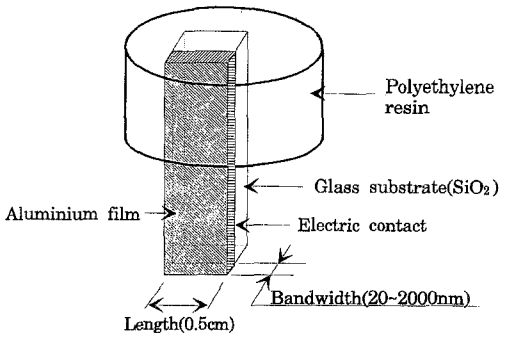


Fig. 1. Schematic representation of aluminium microband electrodes.

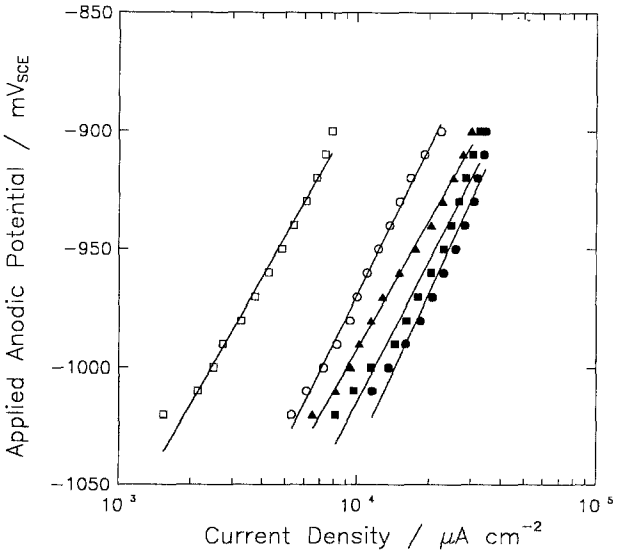


Fig. 2. Anodic polarization of aluminium microband electrodes with different bandwidths in 0.1 M NaOH solution. Bandwidth: (●) 20, (■) 80, (▲) 160, and (○) 500, (□) 2000 nm. Corrosion potential = −1040 mV vs SCE.

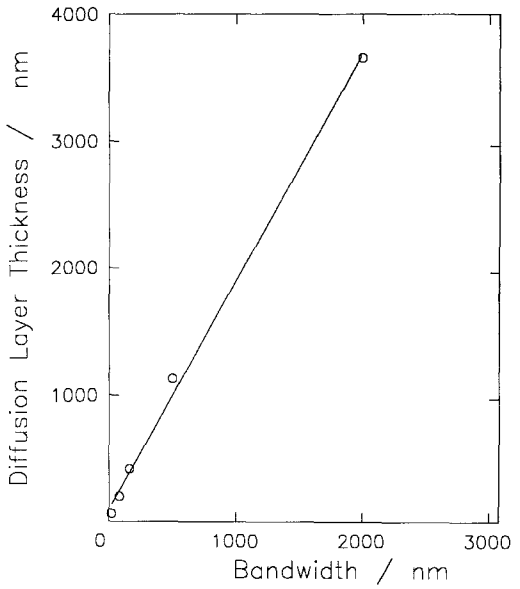


Fig. 3. Plot of diffusion layer thickness against bandwidth.

Inverting Equation 5 yields

$$\frac{1}{i}=\frac{1}{k_aF}\exp\left(\frac{-\alpha_aFV}{RT}\right)+\frac{k_cd}{k_aFD}\exp\left[-\frac{(\alpha_a+\alpha_c)FV}{RT}\right] \quad (8)$$

The reciprocal of the current density is linearly proportional to $d$. The kinetic contribution expressed in Equation 6 can be evaluated from the intercept on current axis, which is provided by

$$\lim_{d\to o}\frac{1}{i}=\frac{1}{k_aF}\exp\left(\frac{-\alpha_aFV}{RT}\right) \quad (9)$$

The derivative of the reciprocal of the current density with respect to diffusion layer thickness is expressed as follows

$$\frac{\partial(1/i)}{\partial d}=\frac{1}{k_aF}\exp\left(\frac{-\alpha_aFV}{RT}\right)\left[\frac{k_c}{D}\exp\left(\frac{-\alpha_cFV}{RT}\right)\right] \quad (10)$$

Inserting Equation 9 into Equation 10 permits evaluation of the second term in the denominator of Equation 5, $k_cd/D\exp(-\alpha_cFV/RT)$, which provides a measure of mass transfer effects (mass transfer index).

The diffusion layer thickness, $d$, for the aluminium microband electrode can be calculated by using a semi-cylindrical diffusion field approximation for the microband electrodes. For a semi-cylindrical electrode [5,8], the diffusion current, $i$, is given by

$$i=\frac{2\pi zFDc^sl}{\ln(4Dt/r^2)} \quad (11)$$

Approximating for a band geometry through $w=\pi r$ if the bandwidth, $w$, is extremely small, Equation 11 becomes

$$i=\frac{2\pi zFDc^sl}{\ln(4\pi^2Dt/w^2)} \quad (12)$$

Assuming a linear concentration profile,

$$i=zFDc^slw/d \quad (13)$$

Use of Equations 12 and 13 yields

$$d=\frac{w}{2}[\ln(4\pi^2Dt/w^2)] \quad (14)$$

The diffusion layer thickness can be obtained as a function of bandwidth from Equation 14 if $D$ and $t$ are given.

## 4. Results and discussion

Figure 2 presents the anodic polarization of the aluminium microband electrodes with different bandwidths in 0.1 M NaOH at room temperature. The anodic current curves follow Tafel-like behaviour with a slope of about 80–90 mV decade$^{-1}$ and show a set of parallel curves. Current density increases with decreasing bandwidth. It should be mentioned that the results are in contrast to those for an electrode of conventional size for which the

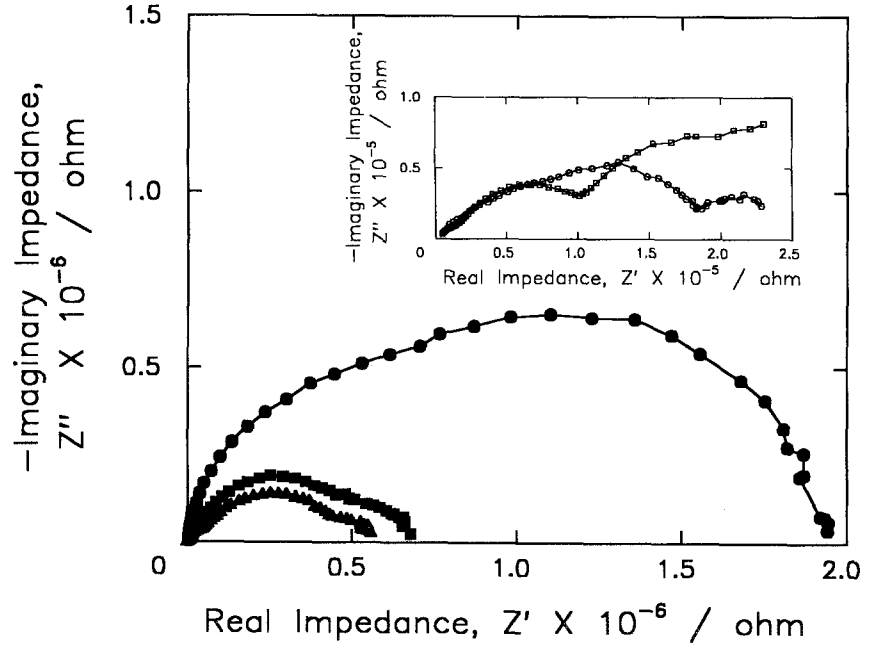


Fig. 4. Nyquist plots obtained from aluminium microband electrodes with different bandwidths, measured at an applied anodic potential of −900 mV vs SCE in 0.1 M NaOH solution. Bandwidth: (●) 20, (■) 80, (▲) 160, and (○) 500, (□) 2000 nm.

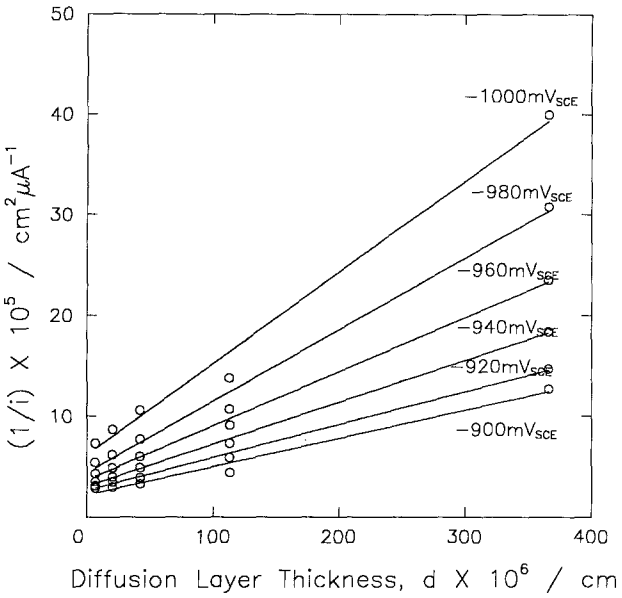


Fig. 5. Reciprocal current density as a function of diffusion layer thickness for various applied potentials.

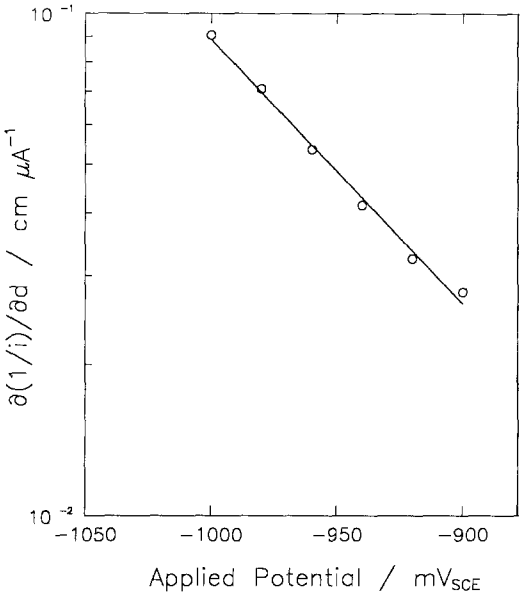


Fig. 7. Plot of derivative of reciprocal current density with respect to diffusion layer thickness against applied potential.

polarization curve is independent of specimen geometry.

It is generally agreed that the semi-cylindrical diffusion contribution to mass transfer towards microband electrodes is more markedly predominant as the bandwidth of the microband electrode decreases [7,8]. In a similar way, a higher dissolution current density from the electrode is expected with decreasing bandwidth in this work.

Provided the current response for the microband electrode is in virtual steady-state in less than 10 s ($t \approx 10$ s), $D = 10^{-5}\,cm^2\,s^{-1}$ [11], the diffusion layer thickness, $d$, near the microelectrode was calculated as a function bandwidth, $w$, from Equation 14. The plot of $d$ against $w$ is given in Fig. 3. In the range of 20 to 2000 nm investigated, the diffusion layer thickness increases linearly with bandwidth. An increase in the diffusion layer thickness gives a lower current density, as presented in Fig. 2.

To ensure the existence of a steady-state diffusion layer, a.c.-impedance measurements were made on the aluminium microband electrodes with different bandwidths at an applied potential of −900 mV vs SCE. The results obtained are shown in Fig. 4. At bandwidths below 500 nm, the Nyquist plots exhibit convective Warburg impedance of a semicircle resulting when a small steady-state diffusion layer exists, whereas at bandwidths of 500 and 2000 nm the plots show increasing impedance at low frequencies, indicating diffusion layer growth with time [12]. Considering a short polarization time-scale (< 10 s), the growth of the diffusion layer thickness is assumed to be negligibly small with time.

Figure 5 shows the reciprocal current density as a

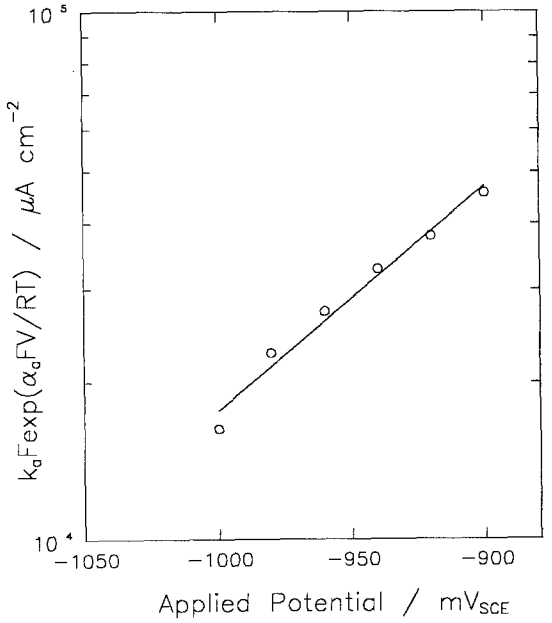


Fig. 6. Kinetic contribution to electrodissolution current density as a function of applied potential.

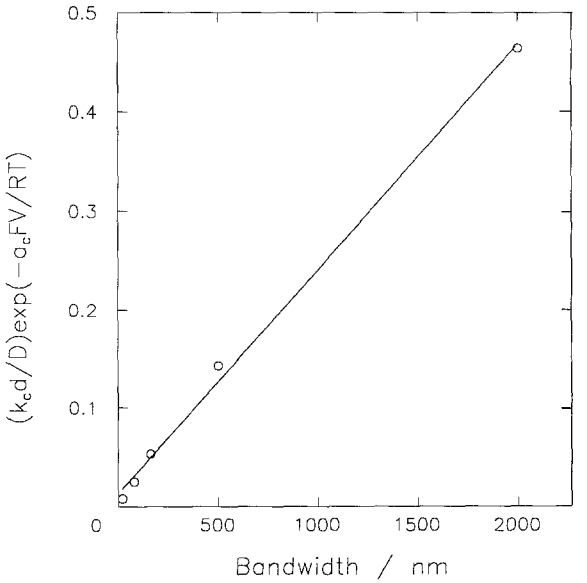


Fig. 8. Mass transfer index as a function of bandwidth for an applied potential of −900 mV vs SCE.

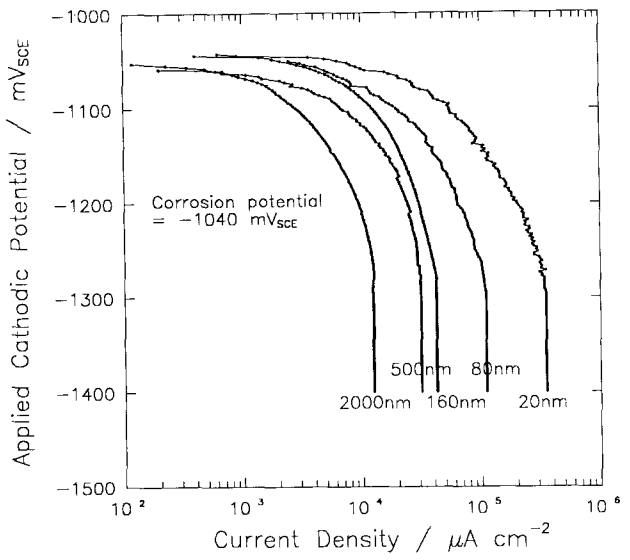


Fig. 9. Cathodic polarization of aluminium microband electrodes with different bandwidths in 0.1 M NaOH solution.

function of diffusion layer thickness for various applied potentials. The reciprocal current density is linearly proportional to the diffusion layer thickness. It follows Equation 8 satisfactorily, indicating that the electrodissolution of the aluminium microband electrodes proceeds by a mixed kinetic-mass transfer controlled reaction. The intercept on the current axis provides a measure of the kinetic contribution to the dissolution current density in the absence of mass transfer effects.

Figure 6 demonstrates the kinetic contribution with respect to applied potential. The result reveals a kinetically-controlled process that would be ordinarily masked by diffusion from a macro-electrode surface.

From the data presented in Fig. 5, the derivative of the reciprocal current density with respect to the diffusion layer thickness is plotted against applied potential in Fig. 7.

The mass transfer index was calculated from the calculated diffusion layer thickness presented in Fig. 3, from the values of the kinetic contribution experimentally determined and presented in Fig. 6, and from the derivative values experimentally determined and presented in Fig. 7. The result is presented as a function of bandwidth in Fig. 8. Within the bandwidth range investigated, the mass transfer index decreases linearly with decreasing bandwidth. This indicates the reduced mass transfer contribution to electrodissolution with decreasing bandwidth. Since a kinetically controlled process is independent of specimen geometry and semi-cylindrical diffusion as compared to laminar diffusion is more predominant with decreasing bandwidth, it is conceivable that reduction in bandwidth decreases the mass transfer index.

The effect of bandwidth on mass transfer was also observed in cathodic polarization of the aluminium microband electrodes, as shown in Fig. 9. The cathodic polarization curves show that the cathodic diffusion limiting current density for hydrogen evolution increases strongly with decreasing bandwidth. The result of a.c.-impedance measurements at an applied cathodic potential of −1350 mV vs SCE is illustrated in Fig. 10; this was found to be similar to that at an applied anodic potential of −900 mV vs SCE. At the cathodic potential, it was very difficult to separate between kinetic and mass transfer effects because of the complexity of the electrode reactions consisting of hydrogen evolution and cathodic corrosion [13, 14]. However, it is clear from the cathodic polarization curves that the smaller bandwidth enhances the semi-cylindrical diffusion.

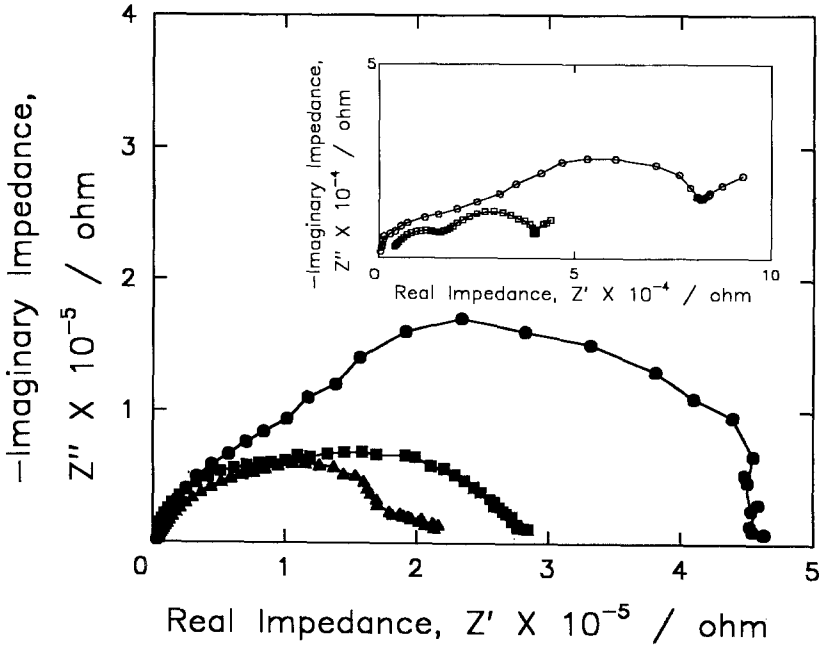


Fig. 10. Nyquist plots obtained from aluminium microband electrodes with different bandwidths, measured at an applied cathodic potential of −1350 mV SCE in 0.1 M NaOH solution. Bandwidth: (●) 20, (■) 80, (▲) 160, and (○) 500, (□) 2000 nm.

## 5. Conclusions

The electrodissolution of aluminium thin film as a microband electrode has been investigated as a function of bandwidth in order to separate between electrode kinetic and mass transfer effects.

The electrodissolution proceeds by a mixed kinetic-mass transfer controlled reaction where mass transfer contribution to the electrodissolution is reduced as the bandwidth is decreased, thereby resulting in a higher current density. These results are considered to be due to the more predominant semi-cylindrical diffusion as compared to the laminar diffusion with decreasing bandwidth. The specimen dimension dependence of electrodissolution suggests that the microband electrode provides a useful tool to distinguish the electrode kinetics from the mass transfer through the electrolyte.

## Acknowledgements

The authors acknowledge the Korea Science and Engineering Foundation for financial support.

## References

[1] S. Asakura and Ken Nobe, *J. Electrochem. Soc.* **18** (1971) 19.
[2] J. C. S. Fernandes, M. G. S. Ferreira and C. M. Rangel, *J. Appl. Electrochem.* **20** (1990) 874.
[3] J. R. Scully, R. P. Frankenthal, K. J. Hanson, D. J. Siconolfi, and J. D. Sinclair, *J. Electrochem. Soc.* **137** (1990) 1365.
[4] O. E. Barcia, O. R. Mattos and B. Tribollet, *ibid.* **130** (1992) 446.
[5] P. M. Kovach, W. L. Caudill, D. G. Peters and R. M. Wightman, *J. Electroanal. Chem.* **185** (1985) 285.
[6] K. Aoki, K. Tokuda and H. Matsuda, *ibid.* **230** (1987) 61.
[7] R. B. Morris, D. J. Franta and H. S. White, *J. Phys. Chem.* **91** (1987) 3559.
[8] C. Chandler, J.-B. Ju, R. Atanasoski, and W. H. Smyrl, *Corrosion* **47** (1991) 179.
[9] R. T. Foley and T. H. Nguyen, *J. Electrochem. Soc.* **129** (1982) 464.
[10] W. H. Smyrl, *ibid.* **132** (1985) 1551.
[11] G. S. Frankel, *Corros. Sci.* **33** (1990) 1203.
[12] J. O'M. Bockris and A. K. V. Reddy, 'Modern Electrochemistry', Vol. 2, Plenum, New York (1970) pp. 1055–9.
[13] Van de Ven and H. Koelmans, *J. Electrochem. Soc.* **123** (1976) 143.
[14] E. Sabeva, I. Dobrewsky and P. Dineff, *J. Appl. Electrochem.* **20** (1990) 986.